SCANNING VOL. 21, 379–386 (1999)

Received June 4, 1999
Accepted August 25, 1999

Influence of Topography and Specimen Preparation on Backscattered Electron Images of Bone

ERIC G. VAJDA, SCOTT HUMPHREY, JOHN G. SKEDROS, ROY D. BLOEBAUM

Bone and Joint Research Laboratory, VA Medical Center, Salt Lake City, Utah, USA

Summary: Backscattered electron (BSE) images of bone exhibit graylevel contrast between adjacent lamellae. Mathematical models suggest that interlamellar contrast in BSE images is an artifact due to topographic irregularities. However, little experimental evidence has been published to support these models, and it is not clear whether submicron topographical features will alter BSE graylevels. The goal of this study was to determine the effects of topography on BSE image mean graylevels and graylevel histogram widths using conventional specimen preparation techniques. White-light interferometry and quantitative BSE imaging were used to investigate the relationship between the BSE signal and specimen roughness. Backscattered electron image graylevel histogram widths correlated highly with surface roughness in rough preparations of homogeneous materials. The relationship between BSE histogram width and surface roughness was specimen dependent. Specimen topography coincided with the lamellar patterns within the bone tissue. Diamond micromilling reduced average surface roughness when compared with manual polishing techniques but did not significantly affect BSE graylevel histogram width. The study suggests that topography is a confounding factor in quantitative BSE analysis of bone. However, there is little quantitative difference between low-to-moderate magnification BSE images of bone specimens prepared by conventional polishing or diamond micromilling.

Key words: bone, backscattered electron imaging, surface topography, white-light interferometry, bone mineral distribution

Address for reprints:

Roy D. Bloebaum
VA Medical Center (151F)
500 Foothill Blvd.
Salt Lake City, UT 84148, USA

Introduction

The mean graylevel of a backscattered electron (BSE) image is a function of the imaged material's mean atomic number (Bishop 1966, Heinrich 1966). In bone samples, mean BSE graylevel intensity correlates with mineral content (Bloebaum *et al*. 1997; Roschger *et al*. 1995; Skedros *et al*. 1993a, b; Vajda *et al*. 1996), making BSE imaging a useful tool for the study of bone mineralization under normal and pathologic conditions. However, other features in addition to mean atomic number influence the BSE signal. Topography, in particular, can lead to local deviations in BSE image brightness (Fig. 1). In studies using BSE image analysis of bone, specimens are often polished or diamond micromilled to suppress topographical effects. It is not clear, however, whether either technique is sufficient to eliminate topographical artifacts in quantitative BSE imaging of bone mineral content.

The most thorough study of topographical artifact in BSE imaging of bone was performed by Howell and Boyde (1994) using a Monte Carlo simulation. They mathematically modeled bone surface topography as a sinusoidal wave with a wavelength of 5 μm and an amplitude of 0.5 μm, where the crests and troughs corresponded to the lamellar patterns in bone tissue. This is reportedly the degree of surface topography one might expect in bone samples prepared by conventional grinding and polishing techniques. The results indicated that the mean graylevel of a peak (e.g., elevated lamella) should have a graylevel that is 17% brighter than what could be accounted for by the atomic number of the sample. Conversely, the mean graylevel of a trough (e.g., depressed lamella) should be reduced by about 14%. The graylevel of the sample taken as a whole should therefore be brighter than could be accounted for by mineral content alone. Howell and Boyde (1994) concluded that lamellae in BSE images could theoretically be accounted for by topography alone, because ". . . topography is more important than any other single factor in determining local variations in the BSE signal reaching the detector."

If this Monte Carlo simulation is correct, then surface topography would introduce errors into any quantitative BSE study, and attempts to interpret quantitatively the relative mineral content differences between microscopic fea-

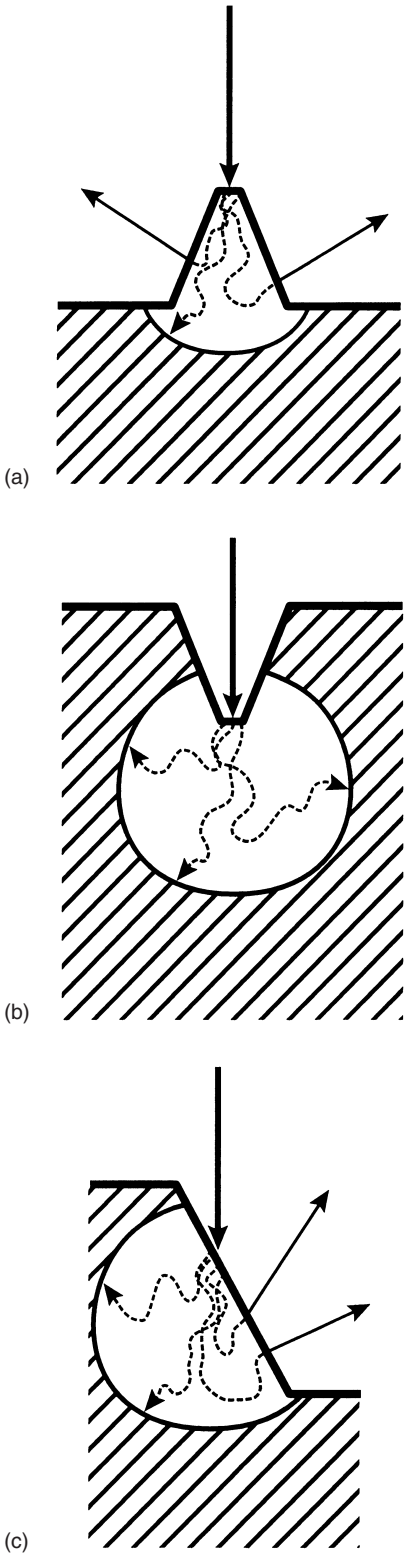

FIG. 1 Diagram of topographical effect on backscattered electron (BSE) imaging. Topographical peaks (a) lead to an increase in the BSE signal topographical troughs, (b) result in a decrease in the BSE signal, and slopes (c) cause a directional increase in the BSE signal. Dotted and solid lines represent electron paths within and outside the specimen, respectively.

tures, such as adjacent lamellae, would be difficult at best. Reducing surface topography using alternate preparation techniques could minimize the problem. It has been argued that diamond micromilling produces a surface with less topographical relief than that produced by standard grinding and polishing methods (Boyde and Jones 1996), but it is unclear whether this would be sufficient for the substantial reduction or elimination of the topographical artifacts. Experimental data examining the differences between these preparation methods and their application to bone specimens are lacking.

The conclusions reached by Howell and Boyde (1994) are dependent on the specific (virtual) electron microscope settings used in their model, as well as on the specific topography given to their sample model. Furthermore, the authors acknowledged that their Monte Carlo model predicts what might occur when using the BSE method to examine a uniform material, and the model does not account for the heterogeneity of bone tissue. Subsequent studies of Monte Carlo methods in low atomic number compounds suggest that there are small errors in the mathematical model (Howell and Boyde 1998, Howell *et al*. 1998). Little quantitative data exist to support the surface topography modeled by Howell and Boyde (1994) or its influence on BSE graylevels in bone. In fact, previous studies using polished specimens have demonstrated very high linear correlations between BSE graylevel and mineral content, leaving little room for surface topography to play an important independent role (Bloebaum *et al*. 1997, Roschger *et al*. 1995, Vajda *et al*. 1996).

The purpose of this study was the experimental examination of the relationship between BSE image graylevels and surface topography using optical phase-shifting and vertical scanning white-light interferometry. The secondary goal of this study was to compare two different methods of bone specimen preparation: diamond micromilling versus conventional grinding and polishing. To achieve these goals, comparative BSE and topographical images were obtained from homogeneous materials prepared with varying degrees of roughness. Second, comparative topographical images were obtained from identical regions of bone specimens prepared by micromilling and by polishing. Finally, quantitative BSE data from bone specimens prepared by micromilling and polishing were compared.

Materials and Methods

Homogeneous Materials

Silicon (nominally > 99% pure; donated courtesy of R. Normann, University of Utah, Dept. of Bioengineering) and magnesium alloy (99.8% pure; 93% Mg, 6% Al, 1% Zn; Johnson/Matthey, Inc., Seabrook, N.H.) were obtained to investigate the effects of topography on BSE images of homogeneous materials. The silicon was manufactured for computer chip applications and was electrochemically pol-

ished to produce a high sheen wafer. The wafer was broken into four pieces. One piece was unprocessed. The second piece was polished with five and then one micron levigated alumina (LECO Corp., St. Joseph, Miss.). The third and fourth pieces were ground with 600 grit and 400 grit sandpaper, respectively. Three pieces of the magnesium wire were processed in a similar manner: one was polished, one was ground with 600 grit sandpaper, and the last was ground with 400 grit sandpaper. No magnesium specimen with surface roughness comparable with the high sheen silicon was available. The silicon and magnesium specimens were mounted with silver paint on aluminum stubs for use in the electron microscope. Backscattered electron images were captured from each silicon and magnesium sample. All samples of like material were placed in the electron microscope at the same time to ensure that electron microscope settings would be identical for all samples of each given substance.

Backscattered electron images were collected with a solid state annular backscatter detector (Tetra, Oxford Instruments, Cambridge, U.K.) configured around the electron beam. These images were captured with a resolution of 512×512 pixels and 8 bits/pixel (256 distinct graylevels) and stored using a computer-controlled image capture and retrieval system (eXL, Oxford Instruments). The BSE images were collected using nine scans and a Kalman frame averaging technique (Oxford Instruments). The accelerating voltage was set to 20 kV, with a probe current of 0.75 nA, an aperture size of 50 μm, and a working distance of 15 mm. Instrument calibration was performed at 20 min intervals by imaging aluminum (99.9999% pure, Johnson/Matthey, Inc.) and magnesium alloy (99.8% pure; 93% Mg, 6% Al, 1% Zn; Johnson/Matthey, Inc.) reference standards following published protocols (Vajda *et al*. 1995). Prior to every image capture, beam current was monitored with an SM-16100 probe current detector (Oxford Instruments) connected to an external picoammeter (Keithley Instruments, Cleveland, Ohio). Fine adjustments of the condenser lens strength were made, as necessary, to insure a stable beam.

It was previously hypothesized (Howell and Boyde 1994) that topography could increase BSE brightness at peaks and decrease brightness at troughs within one microscopic field; therefore, it was felt that measurement of BSE histogram width would provide the most sensitive detection of this phenomenon. Accordingly, the full width at half maximum (FWHM) was calculated for each BSE histogram. All image analyses in this study were performed with custom routines written for public-domain software (NIH Image).

Following BSE imaging, surface topography was examined with optical phase shifting and vertical scanning white-light interferometry (WYKO RST-Plus, WYKO Corp., Tucson, Ariz.). The RST-Plus profiling system utilizes white-light interferometry to produce three-dimensional (3-D) scans of rough surfaces. In an interferometer, light from a reference light source interacts with light reflected off the target surface. The reflected light will vary in phase from the reference beam depending upon the height of the topographical feature from which it is reflected. The interference pattern generated by the two light sources can be processed to reconstruct a 3-D profile of a sample's surface topography (Caber 1993). The horizontal resolution of the interferometer is limited by the optics of the system. For the RST-Plus system at the settings used in the present study, the interferometer had a spatial sampling limit of 0.2 μm. Vertical resolution is even more accurate on an interferometer, with height measurements < 2 nm possible (Caber 1993), which is well below the roughness present in this investigation.

White-light interferometry was performed on each specimen (Michigan Metrology, Livonia, Mich.). The maximum height of the profile (R_t), the root mean square roughness (R_q), and the average roughness (R_a) were calculated for each topographical image. R_t is the vertical distance between the highest and the lowest points on the surface. R_a was calculated for each image using the equation:

$$R_a = \frac{1}{MN} \sum_{k=1}^{M} \sum_{j=1}^{N} \left| Z_{jk} \right| \tag{1}$$

where M is the total number of pixels in the image in the horizontal direction, N is the total number of pixels in the image in the vertical direction, k is the kth horizontal pixel, j is the jth vertical pixel, and Z is the topographical height at the j, kth location. R_q was calculated with the equation:

$$R_q = \sqrt{\frac{1}{MN} \sum_{k=1}^{M} \sum_{j=1}^{N} Z_{jk}^2} \tag{2}$$

where M, N, k, j, and Z are as defined above for Equation 1.

Due to the uniform appearance of these homogeneous samples, it was not possible to identify precisely the same region in BSE imaging and white-light interferometry. However, as there were no distinguishing marks on the surface of each specimen, it was concluded that intraspecimen topographical variability was negligible with respect to interspecimen topographical variability. Specimen average roughness correlated with specimen FWHM using linear regression analysis. Correlation was considered to be statistically significant for $p<0.05$. Throughout the manuscript, data are reported as mean ± SEM.

Effects of Specimen Preparation on Surface Roughness in Bone

Four bones were obtained from three species: human (femur), horse (radius), and deer (antler and calcaneus). Bones were transversely sectioned with a band saw at the mid-diaphysis and a segment of the cortex was taken from each bone. Bone segments were defatted in chloroform and embedded in methyl methacrylate according to published

methods (Emmanual *et al*. 1987). Each bone was diamond micromilled (Reichert-Jung, Germany). During milling, the surface of the bone specimens was lubricated with 50% ETOH. An awl was then used to make straight-line scratches on the surface of each specimen to serve as a grid system for relocating specific regions. Seven fields of view per sample, composed of one osteon and surrounding extraosteonal bone, were analyzed with white-light interferometry. Individual osteons were selected because they represented easily identifiable morphologic features. The maximum height of the profile (R_t), the root mean square roughness (R_q), and the average roughness (R_a) were calculated for each topographical image as described above. In addition, the peak count (number of peaks/unit length) was calculated from each image based on a horizontal and a vertical linescan through the Haversian canal. Peaks were identified based upon peak height as a fraction of average surface roughness (R_a) using algorithms in the WYKO RST-Plus system.

Following white-light interferometry, the samples were polished to introduce topography using five-micron and then one-micron alumina polish (LECO Corp.). Specimens were then reanalyzed with white-light interferometry. Efforts were made to identify the seven osteons within each bone segment that had been previously analyzed. Osteons that could not be conclusively identified following polishing or that showed the presence of surface contaminants were excluded from the study. Interferometry measurements from all fields of view that could be identified with both the polished and the micromilled preparation methods were compared using a paired *t*-test. A p value of < 0.05 was considered statistically significant.

Effects of Specimen Preparation on Backscattered Electron Graylevels

Initially, the same protocol was attempted involving analysis of milled specimens followed by polishing and reanalysis. However, variations in conductive coating thicknesses between the two BSE sessions introduced variation independent of topographical differences. Therefore, an additional bone sample from each of the four bones was obtained, defatted, and embedded in methyl methacrylate. The four bones were glued together with a cyanoacrylate adhesive to form one aggregate specimen block. The specimen block was transversely sectioned with a low speed saw (Isomet, Buehler Ltd., Lake Bluff, Ill.) revealing two opposing faces separated only by the width of the saw blade (~ 0.5 mm). Prior to sectioning, saw marks were made on the periphery of each bone to provide easily identifiable locations on the opposing faces. One surface was diamond micromilled and the opposing surface was manually polished. Both samples were placed in an evaporative coater at the same time and coated with a thin layer of carbon. Both the micromilled and the polished specimen blocks were placed on the stage of the microscope at the same time and analyzed in one operating session. From each bone segment, BSE images were captured from 12 matched regions (same region in both the milled and polished specimen) at 50× and 200× magnifications (7 images at 200×; 5 images at 50×). To ensure consistency within the BSE imaging session, minor adjustments of the condenser lens were made prior to each image capture to ensure that the electron beam did not fluctuate (Vajda *et al*. 1995). The matched region from one specimen block was always imaged immediately after the corresponding region on the opposing specimen block, thus reducing the possibility that instrumental drift would affect the results. For half of the images, the micromilled specimen was imaged first, while the polished specimen was imaged first for the remaining images.

From each BSE image the weighted mean graylevel (WMGL), the FWHM, the skewness, and the kurtosis of the BSE histogram were calculated (Boyce *et al*. 1990, Sokal and Rohlf 1995). Images from the polished and the micromilled preparation methods were compared using a paired *t*-test. A p value of < 0.05 was considered statistically significant.

Results

Homogeneous Materials

Increased surface roughness (R_q) correlated significantly ($p < 0.01$; $r^2 = 0.99$) with increases in BSE histogram FWHM in silicon (Table I, Fig. 2). Surface roughness did not, however, significantly correlate ($p = 0.13$; $r^2 = 0.96$) with BSE histogram FWHM in Mg. The nonsignificant correlation (in spite of a high r^2 value) was probably the result of the small sample size ($n = 3$). The correlation between FWHM and roughness was observed for all of the measured roughness values: R_a, R_t, and R_q. There was one exception—the R_t of magnesium which had been ground

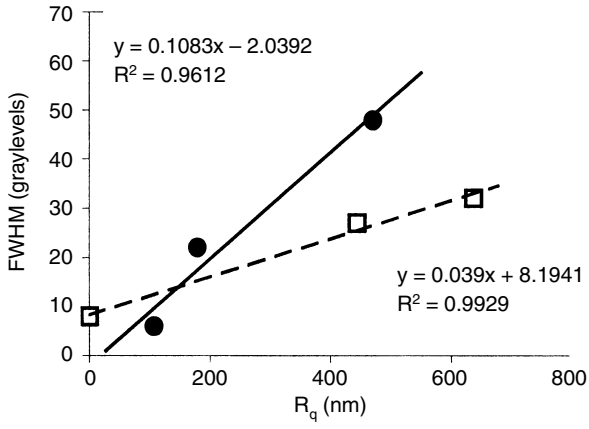

FIG. 2 Correlation between root mean square roughness (R_q) and backscattered electron image full width at half-maximum (FWHM) of magnesium and silicon. Black circles are magnesium, white squares are silicon; polished and high-sheen silicon data points are overlapping.

with 600 grit sandpaper did not follow the trend. R_t is a measurement of the range of surface heights within any image and is thus particularly susceptible to outliers, possibly explaining this anomalous finding. As surface roughness increased, the FWHM of silicon increased at a slower rate than that of magnesium (Fig. 2). As a consequence, it was not possible, in general, to establish a direct relationship between FWHM and surface roughness.

TABLE I Backscattered graylevel and topography data in homogeneous materials

	FWHM (graylevels)	R_q(nm)	R_a(nm)	R_t(nm)
Mg				
Polished	6	108	66	2470
600 grit	22	180	141	1640
400 grit	48	471	374	3880
Si				
Sheen	8	0.6	0.5	5
Polished	8	1	0.7	8
600 grit	27	445	320	7090
400 grit	32	637	493	12510

Abbreviations: FWHM=full width at half maximum, R_q=root mean square roughness, R_a=average roughness, R_t=vertical distance between the highest and lowest points on the surface.

Effects of Specimen Preparation on Surface Roughness in Bone

The surface roughness of polished bone was significantly ($p < 0.0001$) greater than the surface roughness of the same region after micromilling (Table II). This was true no matter which measurement of roughness (R_a, R_q, or R_t) was used, and these results were independent of the species from which the bone sample was taken. There were, however, differences among the species. Average roughness for milled bone was 71 ± 5 nm; average roughness for polished bone was 304 ± 27 nm. In contrast to the roughness measurements, peak count was greater in milled bone specimens than in polished specimens (Table II). Again, these findings were consistent among all four bone samples.

The white-light interferometry images demonstrate that the variations in surface roughness follow bone lamellar patterns (Fig. 3). The osteons, as well as the individual lamellae, are clearly visible in these images. This was true for both milled and polished specimens, indicating that milling does not completely eliminate lamellar patterns. Haversian canals, as well as osteocyte lacunae, were typically topographical troughs. Other morphologic features, such as cement lines, did not typically appear as distinct topographical entities and could not be conclusively iden-

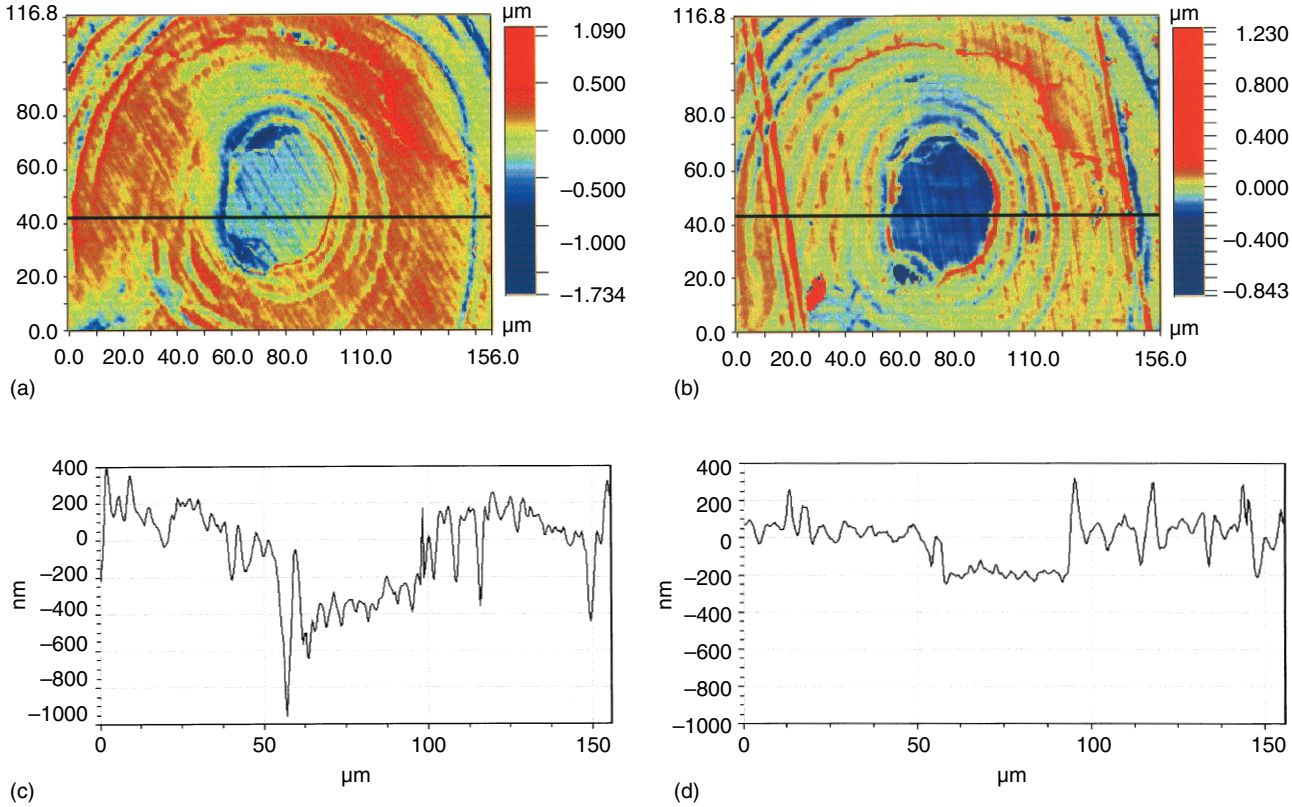

FIG. 3 Comparative pseudocolor white light interferometry images and corresponding line scans from a deer calcaneus after polishing (a,c) and milling (b,d). Lamellar patterns are evident using both preparation techniques, but the topographical undulations are of much greater magnitude in the polished specimen. Scratches as a result of the milling process were often observed on the milled specimens. Similar, more subtle scratches can be seen on the polished specimens. Horizontal field width = 156 μm.

tified in the images. On a linescan (Fig. 3), surface topography followed a quasi-sinusoidal pattern with amplitude approximately equal to 500 nm in polished bone. The same pattern was observed in milled bone, with amplitude approximately equal to 200 nm.

Effects of Specimen Preparation on Backscattered Electron Graylevels in Bone

Quantitative results from both the low and high magnification BSE images were quite similar, and data from both high and low magnification images were pooled to increase statistical power. There was a subtle visual difference between milled specimens versus the same region in polished specimens at higher magnifications (Fig. 4). Lamellae were more pronounced in the polished bone and were particularly evident at sites with lower mineral content (i.e., sites of new bone formation). In spite of this, no statistically significant difference in FWHM was observed for any of the four specimens (Table III). Even after pooling the data from all four bones, FWHM showed only a trend ($p < 0.1$) towards increased width in milled specimens.

The WMGL was significantly greater ($p < 0.0001$) in milled specimens compared with polished specimens for all four bones (Table III). Milled specimens also had a significantly more negatively skewed distribution for all specimens except the deer calcaneus (Table III). Kurtosis was significantly greater in the milled specimens from the horse and human ($p < 0.02$ and $p < 0.0001$, respectively). Although statistically significant differences were observed in histogram shape and placement, the actual magnitude of the effect was relatively small. Comparison of BSE histograms reveals that variations among the specimens were

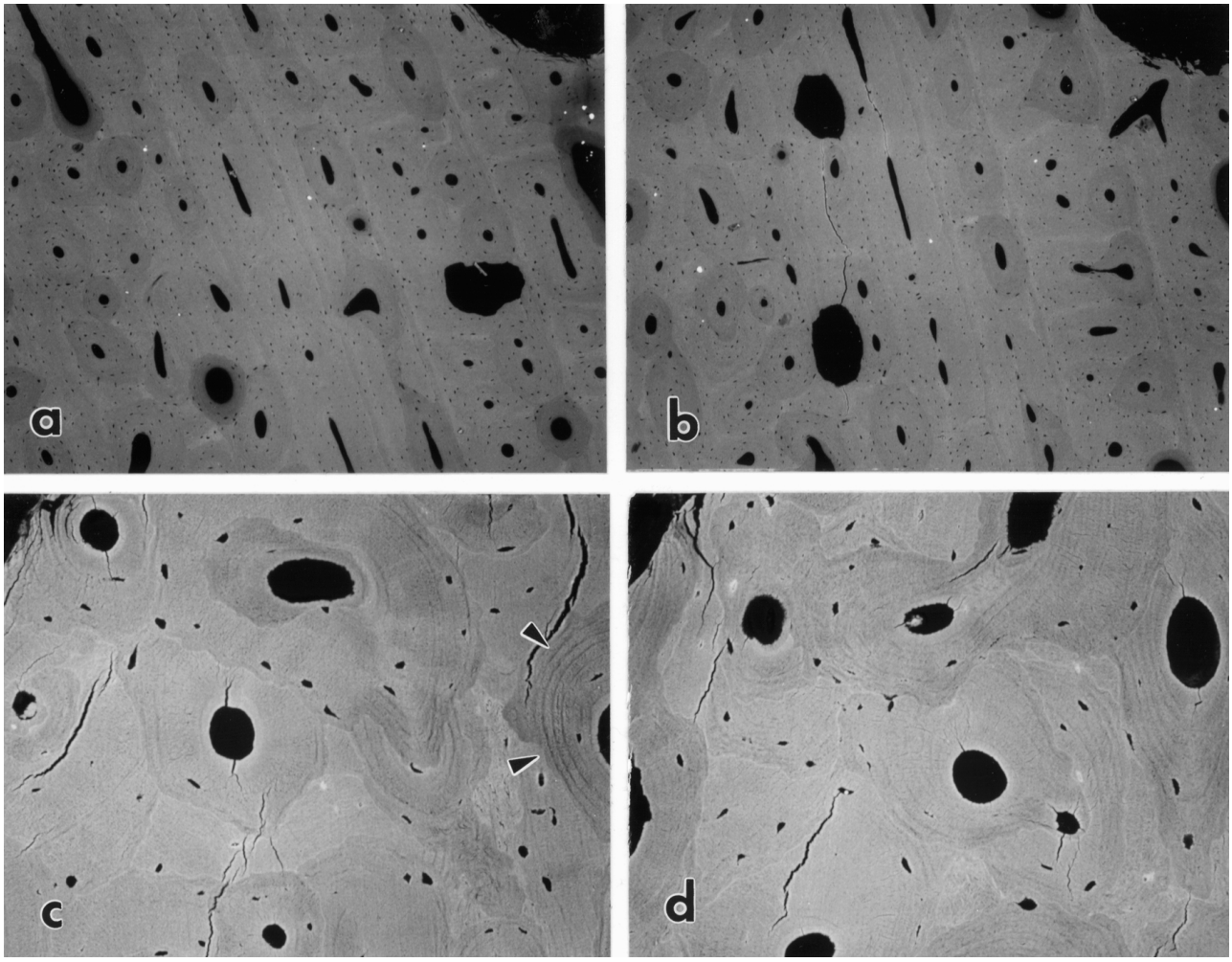

FIG. 4 Low magnification backscattered electron (BSE) images of a horse radius after polishing (a) and milling (b). A negligible difference could be observed between the preparation techniques. Differences in osteon morphology between the two images are due to the anastomoses and bifurcations along the length of an osteon (Cohen and Harris 1958). Horizontal field width = 1.95 mm. In higher magnification images of a human femur, lamellar contrast (arrows) was slightly more evident after polishing (c) compared with milling (d). Some morphologic features, such as cement lines, are more evident in the milled specimens, indicating that cement lines are not a topographical artifact. Horizontal field width = 475 μm.

TABLE II Effects of specimen preparation on surface roughness in bone[a]

	Polished	Milled	p Value
R_a (nm)			
Deer calcaneus	201 ± 25	47 ± 4	0.007
Deer antler	418 ± 54	96 ± 8	0.087
Horse radius	230 ± 29	62 ± 4	0.036
Human femur	338 ± 39	84 ± 3	<0.001
Pooled data	304 ± 27	71 ± 5	<0.0001
R_q (nm)			
Deer calcaneus	360 ± 78	71 ± 4	0.038
Deer antler	654 ± 95	183 ± 19	0.114
Horse radius	321 ± 54	89 ± 3	0.053
Human femur	456 ± 57	113 ± 5	<0.001
Pooled data	455 ± 44	106 ± 10	<0.0001
R_t (nm)			
Deer calcaneus	6354 ± 1376	1119 ± 101	0.015
Deer antler	7486 ± 186	3044 ± 138	0.030
Horse radius	3676 ± 904	1232 ± 152	0.088
Human femur	3726 ± 574	1089 ± 79	0.002
Pooled data	5924 ± 628	1386 ± 181	<0.0001
Peak count (#/mm)			
Deer calcaneus	22.0 ± 3.2	28.1 ± 1.3	0.060
Deer antler	11.7 ± 3.0	21.0 ± 2.4	0.040
Horse radius	21.8 ± 2.7	25.9 ± 3.8	0.092
Human femur	22.2 ± 3.2	26.2 ± 2.6	0.021
Pooled data	20.7 ± 1.8	25.9 ± 1.4	<0.0001

[a]Mean±SEM. Abbreviations as in Table I.

TABLE III Effects of specimen preparation on backscattered electron data in bone[a]

	Polished	Milled	p Value
WMGL (graylevels)			
Deer calcaneus	114.1 ± 0.8	122.8 ± 1.2	<0.0001
Deer antler	74.8 ± 1.3	80.2 ± 1.0	<0.0001
Horse radius	108.0 ± 0.8	115.4 ± 0.7	<0.0001
Human femur	112.9 ± 1.1	118.0 ± 0.8	<0.0001
Pooled data	102.3 ± 2.5	109.0 ± 2.6	<0.0001
FWHM (graylevels)			
Deer calcaneus	35.2 ± 0.5	36.7 ± 0.7	0.08
Deer antler	40.9 ± 0.8	40.5 ± 1.0	0.58
Horse radius	35.6 ± 0.5	36.3 ± 0.6	0.14
Human femur	37.3 ± 0.5	37.8 ± 1.4	0.19
Pooled data	37.3 ± 0.4	37.9 ± 0.4	0.07
Skewness			
Deer calcaneus	–1.00 ± 0.05	–1.07 ± 0.04	0.18
Deer antler	–0.11 ± 0.03	–0.26 ± 0.02	0.001
Horse radius	–0.83 ± 0.05	–0.96 ± 0.04	0.001
Human femur	–0.62 ± 0.04	–0.70 ± 0.05	0.001
Pooled data	–0.64 ± 0.05	–0.74 ± 0.05	<0.0001
Kurtosis			
Deer calcaneus	3.2 ± 0.1	3.11 ± 0.2	0.82
Deer antler	0.4 ± 0.1	0.48 ± 0.1	0.64
Horse radius	2.3 ± 0.1	2.78 ± 0.2	0.02
Human femur	2.0 ± 0.1	2.39 ± 0.1	<0.0001
Pooled data	2.0 ± 0.2	2.18 ± 0.2	<0.01

[a]Mean±SEM. *Abbreviations:* WMGL = weighted mean graylevel, FWHM = full width at half maximum.

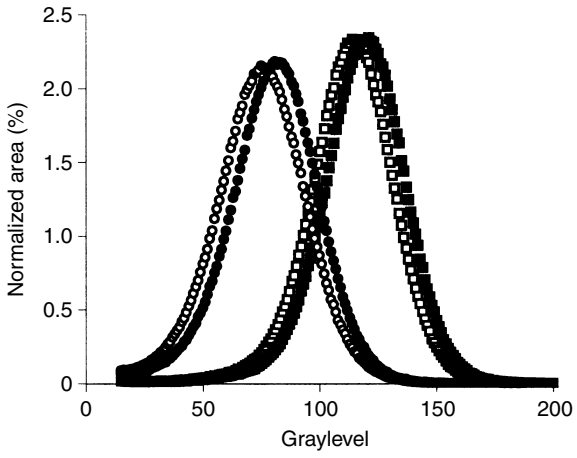

FIG. 5 Backscattered electron graylevel histograms from a deer antler (circle) and a human femur (square), showing minimal differences in histogram shape and small differences in histogram placement between polished (open markers) and milled (solid markers) specimens. Histograms represent summed data from all images captured in the study.

much larger than variations as a result of specimen preparation (Fig. 5). Histogram shapes appeared nearly identical to the unaided eye.

Discussion

The data from the present study clearly identify surface topography as a confounding factor in quantitative BSE imaging. As expected, BSE histogram width was greater in rough than in smooth surfaces in homogeneous materials. Electron microscopists have been aware of this for some time, and the results from very rough preparations of homogeneous materials merely provide quantitative data to describe this phenomenon. The present study also suggests that the relationship between histogram width and surface roughness is specimen dependent. For the same preparation techniques, two materials may have substantially different surface topography and, hence, different BSE histograms. This, too, might be anticipated by microscopists who are familiar with differences in the polishing behavior of various materials.

The present study also demonstrates that surface roughness is significantly reduced by diamond micromilling bone specimens. It is interesting, however, that BSE histogram width was not decreased by micromilling the bone

specimens. This was not predicted by the results from homogeneous materials or the Monte Carlo model of BSE imaging in bone reported by Howell and Boyde (1994). Contrary to these predictions, BSE histogram width was actually broader (nonsignificantly) in milled bone specimens. These results are somewhat surprising, because lamellar patterns are more apparent when visually examining BSE images of polished bone. A possible explanation for this stems from our method of analysis. We analyzed surface roughness using conventional calculations, which are predominantly influenced by the height of the local peaks and troughs. An equally relevant measurement for a BSE image might be the number of local peaks and troughs. Micromilling reduces peak height, but increases the number of peaks (Fig. 6). The result is a more varied graylevel throughout the BSE image in milled specimens.

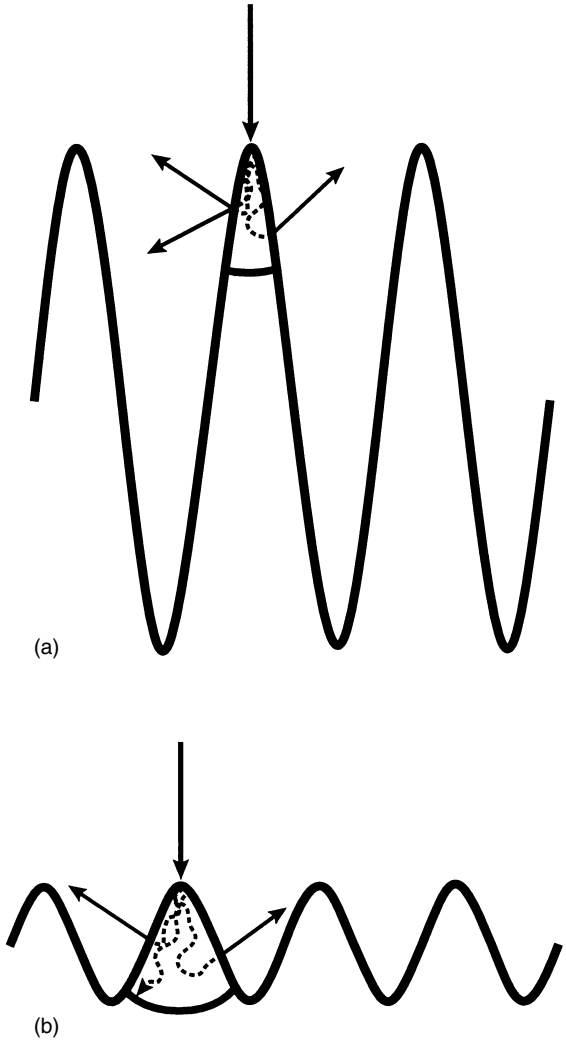

FIG. 6 Schematic representation of surface topography in polished (a) and milled (b) bone specimens. Topography causes a greater change in backscatter fraction at any one peak (or trough) in polished specimens; however, there are more peaks (troughs) in milled specimens. Dotted and solid lines represent electron paths within and outside the specimen, respectively.

In contrast, the larger, less frequent peaks in polished specimens lead to more distinct bands of bright and dark regions in the BSE image, which can be easily detected by the unaided eye (Figs. 4,6).

The discrepancy between the current study and Howell and Boyde's (1994) Monte Carlo model is likely due to the surface topography included in the simulation. Howell and Boyde modeled the surface of polished bone as a sinusoidal wave with an amplitude of 500 nm and compared this with a flat surface. Our data support this as a realistic model of surface topography in polished bone (Fig. 3). It is not possible, however, to obtain perfectly flat specimens, and the study by Howell and Boyde (1994) did not compare topographies based on various specimen preparation techniques. Thus, the discrepancy between our findings and Howell and Boyde's model (1994) stems from the mistaken assumption that reducing surface roughness (peak height) by micromilling will reduce the topographical artifact in quantitative BSE data. The relationship between BSE histogram width and surface topography is clearly more complex and is likely affected by multiple variables such as peak height, peak spacing, and specimen slope. The data from the present study do not support the conclusion that micromilling significantly improves quantitative BSE imaging at low-to-moderate magnifications.

For qualitative BSE studies in bone, micromilled specimens might be preferred because micromilling reduces interlamellar contrast, which is apparently strongly influenced by topography and may not represent a true mineral difference between lamellae. Some investigators (Marotti 1996) have suggested that mineral differences do exist between adjacent lamellae, and it is possible that the residual lamellar contrast observed in BSE images of micromilled specimens is the result of mineral variations. It is equally likely, however, that variations in collagen fiber or mineral crystallite orientation result in irregular polishing and topographic undulations that appear as interlamellar graylevel contrast (Ziv *et al*. 1996). In the absence of perfectly flat specimens, BSE imaging cannot definitively address the issue of interlamellar mineral variations.

Although milling bone specimens reduces interlamellar BSE contrast, it could be argued that polished specimens would be preferred for qualitative BSE analysis. Topography helps to accentuate the lamellar patterns present in bone, making it easier to identify morphologic features (e.g., distinguish woven bone from lamellar bone). The choice of preparation method is largely dependent on the specific goals of the investigator. Investigators must be cautious, however, to avoid interpreting BSE interlamellar graylevel contrast as an indication of interlamellar variation in mineral content.

Previous quantitative studies have shown the BSE signal to be highly correlated with mineral content, and it is unlikely that topography could play a large role in these studies (Bloebaum *et al*. 1997, Roschger *et al*. 1995, Vajda *et al*. 1996). Studies that have shown a high correlation between BSE signal and mineral content were most likely

successful because images were obtained at lower magnifications. In low magnification images, numerous osteons will be present with varying degrees of mineralization. This will undoubtedly lead to variations in histogram shape. The greater mineral variability will play a larger role in BSE signal generation than would be observed from an extremely small field of view. Furthermore, topographical artifact will be averaged over a large area composed of many discrete measurements. The effects of topography on BSE imaging would be more important at higher magnifications, where data could potentially be collected from one or two local topographical features. Topography is a much greater concern in BSE studies that have examined minute fields (Burr *et al*. 1988, Crofts *et al*. 1994, Schaffler *et al*. 1987) and may be more important in specimens with a large proportion of newly formed bone.

Conclusion

The present study supports the findings of the theoretical model described by Howell and Boyde (1994). Interlamellar contrast in BSE images is largely the result of topography present in polished bone specimens. However, in contrast to previous suggestions (Boyde and Jones 1996), diamond micromilling does not eliminate the topographical artifact and does not have a statistically significant influence on BSE histogram width relative to polished specimens. Diamond micromilling reduces specimen roughness, but increases the number of local topographical peaks, resulting in very minor variations in quantitative BSE graylevel data at low-to-moderate magnifications. We conclude that the choice of specimen preparation has minimal influence on quantitative BSE data at low-to-moderate magnifications and that the preparation method used for qualitative studies is largely dependent on the specific goals of the investigation.

Acknowledgments

This project was supported by the Department of Veterans Affairs Office of Research and Development. The authors are grateful for the technical assistance of Pierre Durand, Jr., and the clerical assistance of Gwenevere Shaw.

References

Bishop HE: Some electron backscattering measurements for solid targets. In *Proceedings of 4th Int. Conf. on X-Ray Optics and X-Ray Microanalysis*. Hermann, Paris, 153–158 (1966)

Bloebaum RD, Skedros JG, Vajda EG, Bachus KN, Constantz BR: Determining mineral content variations in bone using backscattered electron imaging. *Bone* 20;485–490 (1997)

Boyce TM, Bloebaum RD, Bachus KN, Skedros JG: Reproducible method for calibrating the backscattered electron signal for quantitative assessment of mineral content in bone. *Scan Microsc* 4;591–603 (1990)

Boyde A, Jones SJ: Scanning electron microscopy of bone: Instrument, specimen, and issues. *Microsc Res Tech* 33;92–120 (1996)

Burr DB, Schaffler MB, Frederickson RG: Composition of the cement line and its possible mechanical role as a local interface in human compact bone. *J Biomech* 21;939–945 (1988)

Caber PJ: Interferometric profiler for rough surfaces. *Appl Opt* 32;3438–3441 (1993)

Cohen J, Harris WH: Three-dimensional anatomy of Haversian systems. *J Bone Joint Surg* 40-A;419–434 (1958)

Crofts RD, Boyce TM, Bloebaum RD: Aging changes in osteon mineralization in the human femoral neck. *Bone* 15;147–152 (1994)

Emmanual J, Hornbeck C, Bloebaum RD: A polymethyl methacrylate method for large specimens of mineralized bone with implants. *Stain Technol* 62;401–410 (1987)

Heinrich KFJ: Electron probe microanalysis by specimen current measurement. In *Proceedings of the Fourth International Congress X-Ray Optics and Microanalysis*. Hermann, Paris, (1966) 159–167

Howell PGT, Boyde A: Monte Carlo simulations of electron scattering in bone. *Bone* 15;285–291 (1994)

Howell PGT, Boyde A: Monte Carlo simulation of electron backscattering from compounds with low mean atomic number. *Scanning* 20;45–49 (1998)

Howell PGT, Davy KMW, Boyde A: Mean atomic number and backscattered electron coefficient calculations for some materials with low mean atomic number. *Scanning* 20;35–40 (1998)

Marotti G: The structure of bone tissues and the cellular control of their deposition. *Ital J Anat Embryol* 101;25–79 (1996)

Roschger P, Plenk H Jr, Klaushofer K, Eschberger J: A new scanning electron microscopy approach to the quantification of bone mineral distribution: Backscattered electron image grey-levels correlated to calcium Ka-line intensities. *Scan Microsc* 9; 75–88 (1995)

Schaffler MB, Burr DB, Frederickson RG: Morphology of the osteonal cement line in human bone. *Anat Rec* 217; 223–228 (1987)

Skedros JG, Bloebaum RD, Bachus KN, Boyce TM: The meaning of graylevels in backscattered electron images of bone. *J Biomed Mater Res* 27;47–56 (1993a)

Skedros JG, Bloebaum RD, Bachus KN, Boyce TM, Constantz B: Influence of mineral content and composition on graylevels in backscattered electron images of bone. *J Biomed Mater Res* 27;57–64 (1993b)

Sokal RR, Rohlf FJ: *Biometry. The Principles and Practice of Statistics in Biological Research* (3rd ed.). W. H. Freeman & Co., New York, 110–115 (1995)

Vajda EG, Bloebaum RD, Skedros JG: Validation of energy dispersive x-ray spectrometry as a method to calibrate backscattered electron images of bone. *Cells Mater* 6;79–92 (1996)

Vajda EG, Skedros JG, Bloebaum RD: Consistency in calibrated backscattered electron images of calcified tissues and mineral analyzed in multiple imaging sessions. *Scan Microsc* 9;741–755 (1995)

Ziv V, Sabanay I, Arad T, Traub W, Weiner S: Transitional structures in lamellar bone. *Microsc Res Tech* 33;203–213 (1996)